Journal of Physics: Conference Series **500** (2014) 182035 doi:10.1088/1742-6596/500/18/182035

Three-dimensional characterisation and simulation of deformation and damage during Taylor impact in PTFE

A D Resnyansky[1], S A McDonald[2], P J Withers[2], N K Bourne[2,3], J C F Millett[3], E N Brown[4] and P J Rae[4]

[1]Weapons and Countermeasures Division, DSTO, PO Box 1500, Edinburgh SA 5111, Australia
[2]School of Materials, University of Manchester, Manchester, M13 9PL, United Kingdom
[3]AWE, Aldermaston, Reading, RG7 4PR. United Kingdom
[4]Los Alamos National Laboratory, Los Alamos, New Mexico 87545, USA

E-mail: anatoly.resnyansky@dsto.defence.gov.au

Abstract. The current work presents Taylor impact experiments interrogating the effect of dynamic, high-pressure loading on polytetrafluoroethylene (PTFE). In particular, X-ray microtomography has been used to characterise the damage imparted to cylindrical samples due to impact at different velocities. Distinct regions of deformation are present and controlled by fracture within the polymer, with the extent of the deformed region and increasing propagation of fractures from the impact face showing a clear trend with increasing impact velocity. A two-phase rate sensitive strength model is implemented in the CTH hydrocode and used for simulation of the problem. The high-pressure phase transition of PTFE into Phase III within the crystalline domains from the polymer at normal conditions is managed by suitable phase transition kinetics within the model. The experimental observations are discussed with respect to the multi-phase model hydrocode predictions of the shock response from Taylor impact simulations. The damage and its progress are shown to correlate well with the onset of the phase transition and its evolution following the impact velocity increase.

1. Introduction

Aerospace, defence and automotive applications of polymers and polymer matrix composites have placed such materials under increasingly more extreme conditions. It is therefore important to understand the mechanical response of these multi-phase materials under high pressures and strain rates. Crucial to this is knowledge of the physical damage associated with phase transformations during loading and the ability to predict this via multi-phase simulation taking thermodynamical non-equilibrium and strain rate sensitivity into account.

In addition, behaviour of PTFE also known as Teflon is of interest due to its abundance of crystalline phases, including the high-pressure Phase III. Mechanical properties of PTFE and their dependence on the crystalline phase content have been studied, e.g., in [1, 2, 3, 4]. The Taylor tests of PTFE rods have been conducted in [5, 6] and novel failure mechanisms with abrupt ductile-brittle transition attributed to the high-pressure transition at a critical impact velocity were studied in [7].

[1] To whom any correspondence should be addressed.

Constitutive modelling of phase transformation in PTFE has previously been considered with a three-phase model in [8]. A hydrocode analysis of the Taylor tests with PTFE, conducted in [9], indicated that the pressure achieved during impact near the failure ductile-brittle transition might be sufficient for the high-pressure phase transition at above the critical velocity of impact. The present work addresses this problem by employing the two-phase model [10] implemented in the CTH hydrocode similar to the implementation described in [11]. The first phase is considered to be PTFE at normal conditions (with the crystalline phase, Phase IV) and the second phase to be the high-pressure crystalline phase, Phase III. The problem is analysed by direct consititutive modelling of the Taylor tests using the model in order to demonstrate the importance of the phase transition within the kinetic approach.

2. Experimental

The Taylor impact tests with PTFE rods with an impact velocity U_0 against a steel anvil [5, 6] have revealed a critical velocity U_c, below which the deformation is typically ductile and above which brittle fracture is observed.

The present Taylor tests employed 45.95 mm long rods with the length to diameter ratio of 5. The critical velocity, U_c, observed in the tests [5, 6] for these rods was found to be 134 m/s. Tomographic reconstructions of the impact surfaces at two impact velocities below and above U_c are shown in figures 1 and 2.

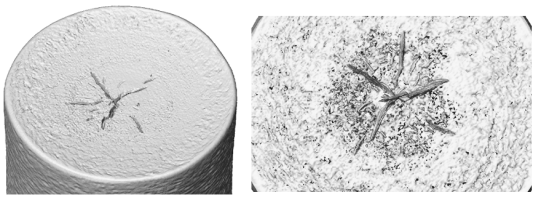

Figure 1. Tomography of the impact surface of the PTFE rod recovered from Taylor test at U_0 = 106 m/s.

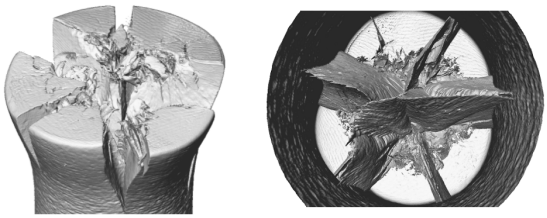

Figure 2. Tomography of the impact surface of the PTFE rod recovered from Taylor test at U_0 = 135 m/s.

From the views of the recovered rods of figures 1-2 a very limited damage area at U_0 = 106 m/s and an extensive brittle damage at a depth from the impact surface can be seen focused in the axial region at U_0 = 135 m/s.

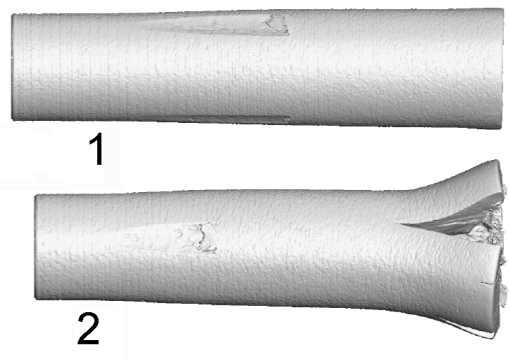

Figure 3. The recovered Taylor test rods at U_0 = 106 m/s (1) and U_0 = 135 m/s (2).

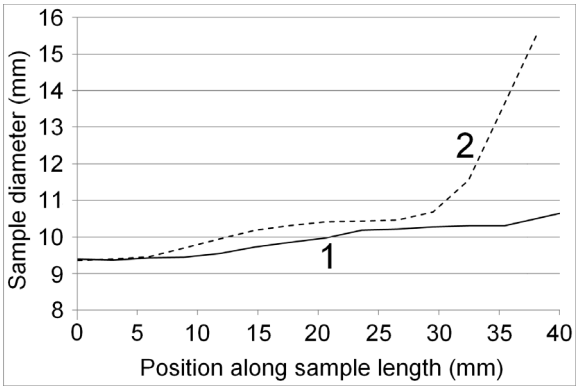

Figure 4. Corresponding side contours of the recovered rods.

Characterisation of the recovered rods in general, reconstructed by three-dimensional X-ray computed tomography, is summarised in figures 3 and 4 at U_0 = 106 m/s (1) and U_0 = 135 m/s (2). The causes for this dramatic change in the damage behaviour will be analysed in the subsequent sections.

3. Model and Model Implementation

A two-phase material model [10] with strength is used for the representation of PTFE as a mixture: the mixed amorphous-crystalline compound at the normal conditions and the high-pressure modification, mainly planar crystalline structure, Phase III.

The model [10] incorporates the conservation laws, the shear strain rheological laws and the constitutive equations managing the inter-phase exchange parametres. The constitutive equations are closed with the help of the kinetic evaluation methodologies [8, 10], which include the following set. The mass exchange rate for the parameter of the mass concentration of the first phase is a simplified version of the phase transition kinetic taken from [8] with the transition initiating pressure, p_{cr}, slightly decreasing with temperature in accordance with the PTFE phase diagram [1]. The compaction rate for the parameter of the volume concentration of the first phase is evaluated from the inter-phase compressibilities similar to the phase transition treatment in iron simulated in [10]. The heat exchange rate for the heat exchange parameter (inter-phase entropy disbalance) is obtained from evaluation of heat equilibration between phase clusters similar to [8, 10]. The stress relaxation functions for parameters associated with the shear strain rheology and inter-phase strain work exchange are obtained from two yield stresses (for example, the dynamic, Y_d, and static, Y_s) versus strain rates for each of the two phases.

The model equations are closed with the equations of state (EOSs) for each of the phases in the form of internal energy as a function of density, deviatoric strains and entropy. The mass weighted internal energy, e, for the material represented by a mixture of the phases, is the EOS for the two-phase material. Differentiating e, the thermodynamic rules allow us to calculate all dependent thermodynamic parametres, including pressure, affinity of the Gibbs energies (the chemical potential governing the phase transition), the compaction rate, shear stresses, the strain work exchange rate, temperature, and temperature disbalance.

The model implementation in the CTH hydrocode [12] follows the same steps as described in [11] for two-phase porous material model. EOS input parameters and yield limits are assigned at two specified strain rates for each phase. Specification of the input parameters for the phase transition, compaction and heat exchange kinetics agrees with the algorithm [8].

The peculiarity of the present implementation for two condensed phases is a deviatoric stress update for the phases concurrently with the mass and volume concentration updates. Update of the remaining external variables is performed at the end of the Lagrangian step in contrast to the implementation in [11].

4. Numerical results

The mechanical characteristics are taken from [5] for PTFE under normal conditions with the high-pressure phase corrections resulting in a 20% increase of the Young modulus, E, and the shear modulus, G. A summary of the data, including initial density ρ, for the two pre-selected phases of the PTFE model is: ρ_1 = 2.17 g/cm^3, E_1 = 1.077 GPa, G_1 = 0.36 GPa, ρ_2 = 2.355 g/cm^3, E_2 = 1.4 GPa, G_2 = 0.475 GPa. The static and dynamic yield limits are chosen for the first phase as Y_s = 60 MPa at $d\varepsilon/dt = 10^{-3}$ 1/s; Y_d = 90 MPa at $d\varepsilon/dt$ = 3200 1/s with a 30%-increase in the yield limits for the second phase. The kinetic parameter p_{cr} varies from 0.45 GPa at room temperature down to 0.35 GPa at 60 deg C.

To take a closer look at the phase transition process with the present two-phase representation of PTFE using the kinetics chosen, a one-dimensional analysis is conducted for the inverse set-up (impact of 10 mm PTFE sample by 5 mm steel anvil). In figure 5, the right section between the dashed lines (initially, between 0.6 and 1.6 cm) is occupied by PTFE and the left section (initially, between 0.1 and 0.6 cm) by steel flyer plate. The space distributions of pressure and mass concentration of the first phase (PTFE at the ambient conditions) in the plane impact assembly at the impact velocity U_0 are

drawn in figure 5 at t = 2 μs (1) and 4 μs (2). Displacement of the flyer plate during the 2 μs-interval, which is larger at a larger U_0, is seen as a displacement of the dashed lines of the left section. No phase transition is observed at U_0 = 106 m/s and a clear phase transformation following the main wave transferring the material to the Hugoniot state corresponding to the impact pressure is observed at U_0 = 500 m/s. The material exhibits the phase transition effects at U_0 between 106 m/s and 135 m/s. In the vicinity of this threshold, the phase boundary seen as the mass concentration jump is kinetically driven and is nearly stationary. The pressure below or nearly p_{cr} is achieved by a precursor merging with the main wave in this range of loads. The phase boundary starts moving with the main wave when pressure increases. In that case, the main wave and the multi-step wave structure have clearly formed (e.g., see figure 5 for U_0 = 200 m/s).

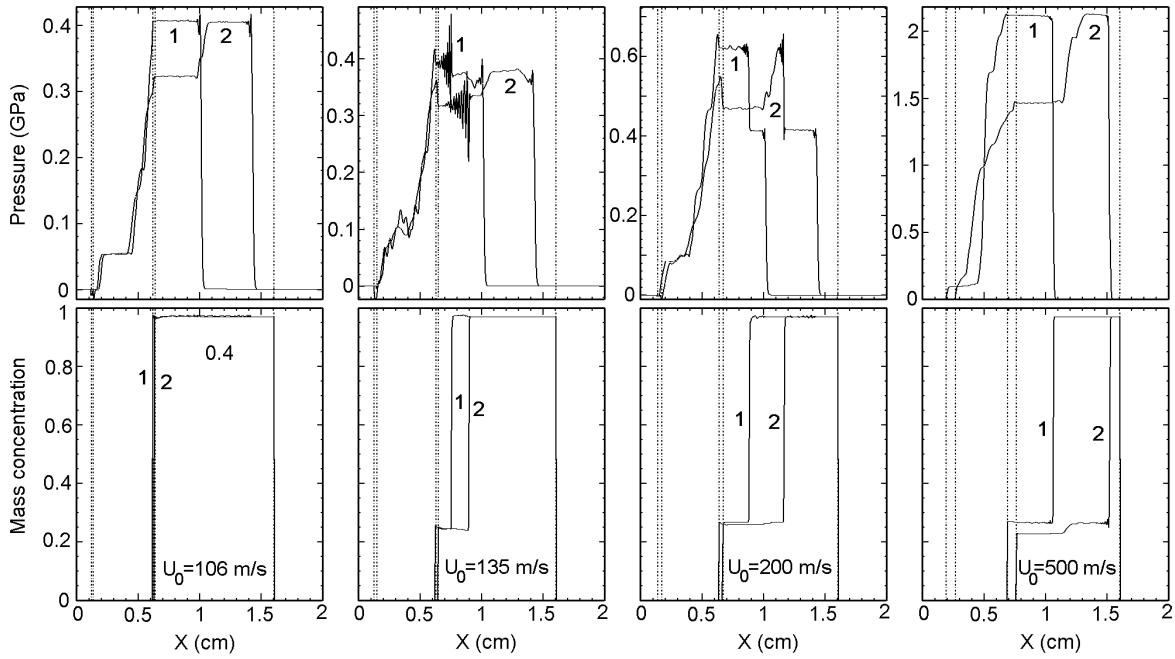

Figure 5. The phase transition development with increasing impact pressure.

It should be noted from the above analysis that the phase transition, taking place at U_0 = 135 m/s, is not clearly apparent as seen in the pressure profiles and becomes clearer at higher loadings. This kinetic behaviour substantiates the choice of p_{cr} for the phase transition kinetic to be lower than the usually experimentally apparent phase transition pressure varying with temperature between 7 and 5 kbar, which is well known from the phase diagram of PTFE [1]. Another factor contributing to stagnation of the phase boundary is the interaction of the incoming shock wave with the overcoming release waves. Manifestation of the phase interface in the VISAR traces, appearing as the stagnating PIR wave at the pressure drop, has been observed in [13] and modeled with the present model in [10].

The Taylor tests described in the second section of the paper have been simulated in a two-dimensional set-up using CTH with the implemented two-phase model. At the initial stage of the impact process, the pressure is focused at the axis near the rod-target interface. Pressure in PTFE exceeds p_{cr} at a depth from the rod-anvil interface for the case U_0 = 135 m/s seen as the dark gray zones for the pressure contours in figure 6. For the case of U_0 = 106 m/s, pressure slightly exceeds p_{cr} only in the direct vicinity of the anvil region. It should be kept in mind that due to the lateral release waves the wave picture is complicated in contrast to the one-dimensional analysis and development of the phase boundary tends to stagnate more easily. Therefore, after this initial stage the pressure in this region is mainly below p_{cr} and the phase interface is practically stationary, similar to the results of the one-dimensional calculations.

The final stage of the calculation when pressure in the rod is reduced to the elastic values is shown in figure 7. The rod shapes for the cases of U_0 = 106 m/s and U_0 = 135 m/s qualitatively agree with the post-impact contours of figure 4. The maximal diameter at the impact face for the case U_0 = 135 m/s is below that observed. However, the petaling mode of fracture has not been simulated. Therefore, this divergence is reasonable to prevent violation of the mass conservation law.

The pictures below show corresponding contours of a failure parametre introduced in the model as an auxiliary tracing parameter characterizing the gradient (jump) of the mass concentration. This failure is consistent with a volume change at the phase transition.

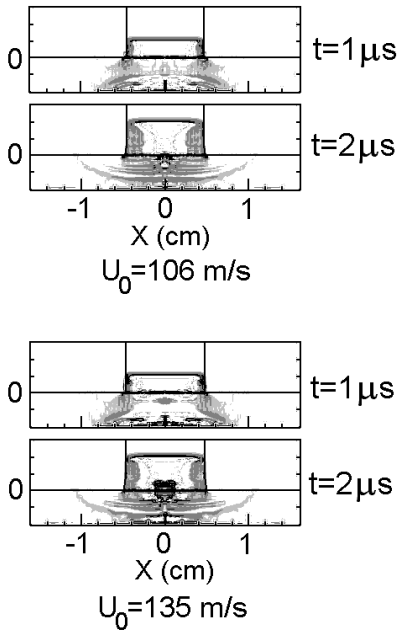

Figure 6. Calculated pressure contours at the initial stage of the rod-anvil interaction.

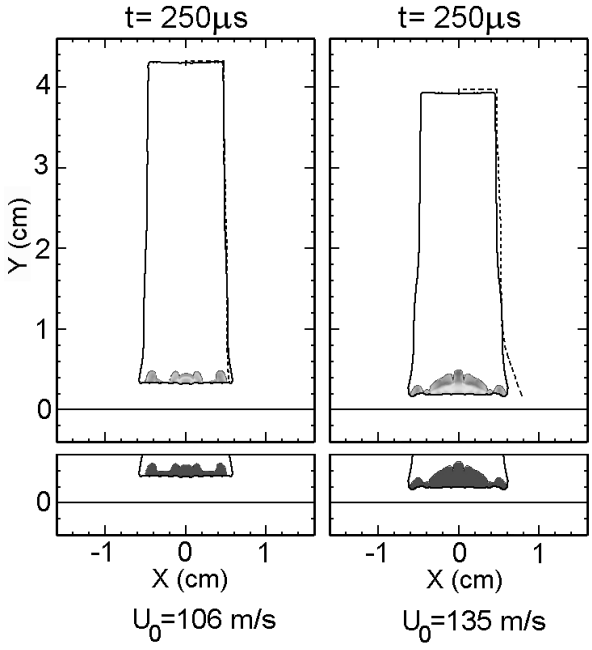

Figure 7. CTH calculated phase transition and 'fracture' parameter contours of the modelled PTFE after the rod rebound from the anvil.

Comparison of observed shapes of the recovered Taylor test samples (dashed contours from figure 4) with the calculation results shows a reasonable agreement given the uncertainties in the mechanical properties of PTFE and, specifically, those of the high-pressure phase. Additionally, the discrepancy seen at the higher velocity is consistent with the viscoelastic relaxation observed in recoved polymer Taylor impact specimens relative to *in situ* high-speed photographic observations [14, 15, 16].

5. Conclusions

A two-phase model implemented in CTH has allowed us to observe and analyze phase evolution in the Taylor impact test using PTFE rods. The analysis shows that pressure in the Taylor test with an impact velocity in the vicinity of the critical velocity characterizing the observed ductile-brittle fracture transition, is close to the phase transition threshold. The shock propagation is followed by a phase boundary degenerating to the stagnating phase interface in PTFE rod at this impact velocity.

Correlation of the high-pressure phase (Phase III) domain with the experimentally observed failure zone confirms that the high-pressure transition might be a cause of the failure since there is a volume contraction in the high-pressure phase.

The yield stress and modulus variations with temperature have not been considered in the present calculation and may result in the observed divergence of the recovered rod shape. Elastic reverberations continue for a long time after the rebound of the rod from the anvil, which also results

in some uncertainty in calculations for the recovered rod. The slightly reduced diameter of the rod at the impact face in the brittle facture regime is a consequence of the continuum treatment of the PTFE material in the calculation, which prevents the rod end from flattening by petalling during fracture.

References

[1] Rae P J and Dattelbaum D M 2004 *Polymer* **45** 7615
[2] Rae P J and Brown E N 2005 *Polymer* **46** 8128
[3] Brown E N, Rae P J and Gray G T 2006 *J. Phys. IV France* **134** 935
[4] Brown E N, Rae P J, Dattelbaum D M, Clausen B and Brown D W 2008 *Exp. Mech.* **48** 119
[5] Bourne N K, Brown E N, Millett J C F and Gray G T III 2008 *J. Appl. Phys.* **103** 074902
[6] Rae P J, Gray G T, Dattelbaum D M and Bourne N K 2004 *AIP Conf. Proc.* **706** 671
[7] Brown E N and Dattelbaum D M 2005 *Polymer* **46** 3056
[8] Resnyansky A D, Bourne N K, Millett J C F and Brown E N 2011 *J. Appl. Phys.* **110** 033530
[9] Rae PJ, Brown EN, Clements BE and Dattelbaum DM 2005 *J. Appl. Phys.* **98** 063521
[10] Resnyansky A D 2010 *J. Appl. Phys.* **108** 083534
[11] Resnyansky A D 2012 *CTH Implementation of a Two-Phase Material Model With Strength: Application to Porous Materials: Report DSTO-TR-2728* (Edinburgh, Australia: Defence Science and Technology Organisation)
[12] Bell R L, Baer M R, Brannon R M, Crawford D A, Elrick M G, Hertel E S Jr., Schmitt R G, Silling S A and Taylor P A 2006 *CTH user's manual and input instructions version 7.1* (Albuquerque, NM: Sandia National Laboratories)
[13] Barker L M and Hollenbach R E 1974 *J. Appl. Phys.* **45** 4872
[14] Brown E N, Trujillo C P and Gray G T 2007 *AIP Conf. Proc.* **955**, 691
[15] Furmanski J, Trujillo C P, Martinez D T, Gray G T III and Brown E N 2012 *Polymer Testing* **31**, 1031
[16] Furmanski J, Cady C M and Brown E N 2013 *Polymer* **54** 381